

Searches for Proton Decay and Superheavy Magnetic Monopoles

B. V. Sreekantan *Tata Institute of Fundamental Research, Homi Bhabha Road, Colaba, Bombay 400005*

(Invited article)

1. Motivation

1.1 Proton Decay

By the mid-thirties of this century it had become clear that all matter, consisting of molecules and atoms, was reducible to just three fundamental particles—the proton, the neutron and the electron. The proton and the electron were regarded as absolutely stable and the neutron though unstable in its free state was stable when bound inside the nucleus. The discovery of the positron, the anti-particle of the electron, established the Dirac theory of the electron. This theory was based on quantum mechanics and the special theory of relativity, and could explain the behaviour of charged particles in passing through matter and almost all aspects of emission and absorption of radiation by molecules and atoms. The finer radiative effects, however, needed the development of quantum electrodynamics (QED) for their explanation. In QED, the simplest example of a gauge theory, the photon or quantum of radiation mediated the electromagnetic force. At this stage the only things which seemed to need further clarification were the nature of the nuclear force—that bound the protons and the neutrons together inside the nuclei—and the presence of a very penetrating component in the cosmic radiation, and the occurrence of atmospheric cascade showers.

The discovery of the muon in 1937 solved the problem of the penetrating radiation and the discovery of the pion in 1947 was a great boost to the theory of nuclear forces based on Yukawa's ideas. The discovery of π^0 mesons (which are produced along with charged pions), and their decay into γ rays and muons solved the problem of cascade showers. The β -decay of the neutron and of other radioactive substances led to the postulate of a massless spin $-\frac{1}{2}$ particle—the neutrino. Just when one was getting the feeling that the nuclear forces were becoming tractable, and all physical phenomena could be elegantly explained on the basis of a few elementary particles, things began to happen rapidly in cosmic-ray research, and later at higher and higher energy accelerators, that changed the whole course of this area of physics. A large number of extremely unstable fundamental particles were discovered with lifetimes ranging from 10^{-8} s to 10^{-22} s and with masses extending upto 10 GeV; some of them were fermions and some were bosons, and some of them required additional quantum numbers like strangeness, charm *etc.* Their number kept on increasing with the increase in the energy of the accelerators.

These particles were classified on the basis of their masses as leptons, the light ones; mesons of medium mass, and baryons, the heavy ones. Among these the strongly interacting particles are known as hadrons. Examples of hadrons are baryons, *e.g.* the proton, the neutron, Λ^0 , Σ^+ *etc.* and mesons, *e.g.* the pion, the kaon, ρ , ω *etc.* The

electron, the positron, μ^\pm , τ^\pm and neutrinos ν_e , ν_μ , ν_τ make up the lepton family. Each particle has a corresponding anti-particle.

While classification of the hadrons (whose number rose to hundreds) according to their grouping into charge multiplets, super-multiplets and the eightfold way *etc.* brought some order into this jungle of fundamental particles, the real simplification and progress however came with the introduction of the ‘quark’ model and its development into the theory known as ‘quantum chromodynamics’ (QCD). In this picture all the baryons and mesons are composites of more elementary entities called ‘quarks’ and their antiparticles ‘antiquarks’. There are six ‘flavours’ of quarks, and in each flavour there are three varieties distinguished by their ‘colour’. The properties are given in Table 1 which also illustrates the quark compositions of some of the hadrons.

According to the quark model, the proton is a composite of two up-quarks and a down-quark (uud), the three quarks having different colours such that they combine to make the proton ‘colourless’. The pion, say the π^- , is a combination of a quark and an antiquark ($d\bar{u}$), and so on. Thus the hundreds of hadrons reduce to combinations of just 18 quarks and 18 antiquarks. Clearly the spin, the charge and the baryon number of quarks have been adjusted to give the observed properties of the combinations—the mesons and the baryons. The strange (s), the charmed (c), the top (t), and the bottom (b) quarks are necessary to account for the new particles K , Λ , Ψ/J , Y , *etc.* which have nonzero values of special quantum numbers like the strangeness.

In QCD, the quark-quark forces are mediated by the exchange of eight massless vector bosons called ‘Gluons’. Each gluon carries a colour charge, *i.e.* the strong charge. The absorption or emission of a gluon by a quark changes its colour. This is a major difference between QED and QCD. In QED, the charge of a particle is unchanged by emission or absorption of a photon since the photon carries no electric charge. An important property of the QCD force is that it depends on the momentum carried by the gluon, and the higher the momentum the weaker the force. This feature of the force has two important consequences. It makes the quarks behave as free particles at extremely short distances—the so-called property of asymptotic freedom. It is also believed that the force increases with distance leading to permanent confinement of quarks within the hadrons. Enormously large energies would be required to free the quarks from the particles in which they are bound. In such attempts, quark-antiquark

Table 1. Properties assigned to the different flavours of quarks.

| Flavour | Spin | Charge | Baryon number | Charm number | Strangeness number | Mass |
|---------|------|-----------------|---------------|--------------|--------------------|--------------|
| d | 1/2 | $-\frac{1}{3}e$ | 1/3 | 0 | 0 | 300 Mev |
| u | 1/2 | $\frac{2}{3}e$ | 1/3 | 0 | 0 | 300 MeV |
| s | 1/2 | $-\frac{1}{3}e$ | 1/3 | 0 | 1 | 500 MeV |
| c | 1/2 | $\frac{2}{3}e$ | 1/3 | 1 | 0 | 1500 MeV |
| t | 1/2 | $\frac{2}{3}e$ | 1/3 | 0 | 0 | Not seen yet |
| b | 1/2 | $-\frac{1}{3}e$ | 1/3 | 0 | 0 | 5000 MeV |

Typical combinations: $p = uud$, $\Omega^- = sss$, $\Delta^+ = uuu$, $\pi^- = d\bar{u}$, $\Delta^- = ddd = d_r d_g d_b$, $K^+ = u\bar{s}$, $Y = b\bar{b}$, $D = c\bar{u}$, $\bar{c}d$, $F = c\bar{s}$.

combinations would be generated resulting in the emergence of bound particles rather than free quarks. This would explain the anomaly that free quarks have not been observed so far in searches with cosmic rays and accelerators. QCD which is a gauge theory has been successful in explaining many of the features of high-energy interactions observed at the accelerators. The nuclear force that binds the protons and neutrons in the nuclei in this scheme, emerges as a residue of the quark-quark forces.

Another exciting development that has taken place in the last two decades is the unification of the weak and electromagnetic forces, again as a gauge theory. While in QED the electromagnetic interactions are considered to be mediated by photons, the weak interactions in the electro-weak theory are assumed to be mediated by massive intermediate vector bosons W^\pm and Z^0 . As was already noted in the context of QCD, in non-Abelian gauge theories (of which the electro-weak is also one) the identity of the particle is changed when the mediating bosons are absorbed or emitted.

An electron may emit a charged boson (W^-) and get transformed into a neutrino. In the unified electro-weak theory, the photon, the W^\pm , and the Z^0 belong to the same family. At extremely high energies ($> 10^{11}$ GeV) the strength of their interactions becomes identical. The force is then long range and the weak coupling constant is the same as that of the electromagnetic force. Below this energy, due to a mechanism known as spontaneous symmetry breaking, the W^\pm and Z^0 acquire mass, and the long-range character of the weak force becomes an extremely short-range one. The Weinberg–Salam electro-weak theory made specific predictions—(i) the existence of neutral currents involving the exchange of the neutral Z^0 particles, and (ii) the mass of W^\pm as 81 GeV and that of Z^0 as 93 GeV. Experimentally, the neutral currents were established in 1974. The W^\pm and Z^0 with precisely the masses predicted, were discovered at the CERN $\bar{p}p$ Collider in 1983, thus giving the final stamp of success to the electro-weak theory.

The initial success of the gauge theories in unifying electromagnetic and weak forces propelled many theorists (Pati & Salam 1973; Georgi & Glashow 1974; Georgi, Quinn & Weinberg 1974) to explore the feasibility of constructing a single gauge theory of all the three forces—the strong, the weak and the electromagnetic—particularly since strong interactions had been incorporated into a successful gauge theory, *i.e.* QCD. Pati (1983) gives an excellent account of the historical development, the current status and future prospects of these theories with an exhaustive list of references. Experimental support for such unification came from the inelastic scattering experiments of electrons and neutrinos on nucleons, and from the study of the behaviour of coupling constants of strong and electro-weak interactions with increasing energy transfer. In these theories, all the coupling constants converge to a common value at the unification energy of 10^{15} GeV as shown in Fig. 1.

While there are a number of models $SU(4)^4$, $SU(5)$, $SO(10)$, E_6 , E_7 , $SU(7)$ *etc.*, named after the mathematical group of symmetries that connect the forces, in the following we shall consider the simple $SU(5)$ model to illustrate the general direction of progress.

In the $SU(5)$ model, there are 24 vector bosons that couple 24 different currents. The photon, W^\pm , Z^0 and the 8 gluons of QCD, constitute a subset of 12 vector bosons. The other 12 are new massive leptoquarks (X , Y) which carry both flavour and colour, three of charge $-(1/3)e$ and three of charge $-(4/3)e$ and the six corresponding antiparticles. It is the leptoquarks that bring about the interaction between the quarks and leptons and their mass is around 10^{15} GeV/ c^2 , the unification energy. The two important predictions of the grand unification theories (GUTs) are: (i) the proton (and the

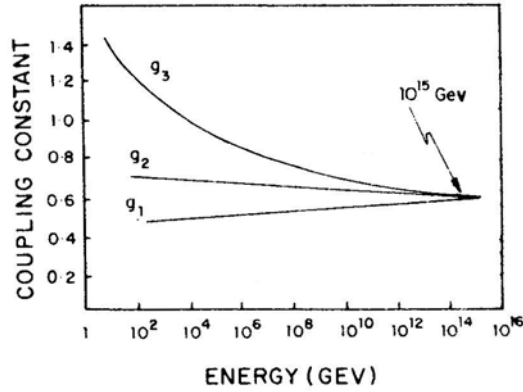


Figure 1. The energy dependence of the strong and electroweak coupling constants showing convergence at $\sim 10^{15}$ GeV. While g_3 is the strong coupling constant, g_1 and g_2 are linear orthogonal combinations of the electromagnetic and weak coupling constants.

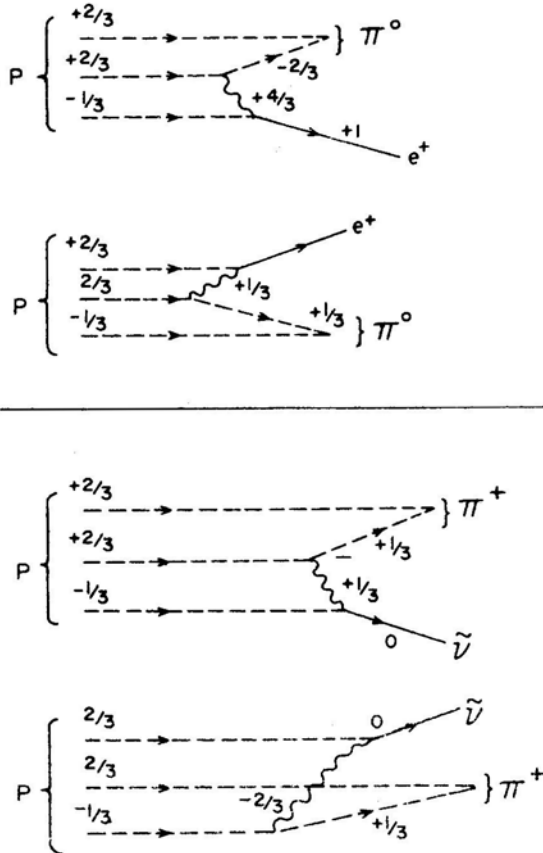


Figure 2. Emission and absorption of leptoquarks through quark-quark interactions leading to proton decay.

neutron even if it were bound) must decay violating baryon number conservation, and (ii) super-heavy magnetic monopoles must exist.

The typical mechanism of proton decay brought about by the emission and absorption of leptoquarks by quarks is illustrated in Fig. 2. For example, by the emission of a leptoquark of charge $(4/3)e$, the quark with charge $(2/3)e$ transforms into an antiquark of charge $-(2/3)e$, which together with a quark of charge $(2/3)e$ becomes a π^0 . The emitted $(4/3)e$ leptoquark is absorbed by the $-(1/3)e$ quark of the proton and transformed into a positron. A leptoquark which plays this dual role is called a diquark. Note that the electric charge and colour are conserved in these reactions throughout.

The probability of this type of interaction depends on the mass of the X particle. In fact, the lifetime for decay is proportional to the fourth power of M_X , the mass of the X -particle *i.e.*,

$$T_p = \frac{k}{\alpha^2} \cdot \frac{M_X^4}{m_p^5}$$

where $k \sim 1$ and $\alpha = 0.02$. If $M_X = 2 \times 10^{14}$ GeV/ c^2 then $T_p = 3 \times 10^{29}$ yr.

Table 2. Predictions for branching ratios for proton and neutron decay into the major two-body decays in the SU(5) model.

Proton decay:

| Mode | (a) | (b) | (c) | (d) | (e) | (f) | | |
|------------------|-----|-----|-----|-----|-----|-----|-----|----|
| | REC | NR | R | R | R | NR | REC | R |
| $e^+ \pi^0$ | 31 | 37 | 9 | 13 | 31 | 36 | 40 | 38 |
| $e^+ \rho^0$ | 15 | 2 | 21 | 20 | 21 | 2 | 7 | 11 |
| $e^+ \eta$ | 11 | 7 | 3 | .1 | 5 | 7 | 1.5 | 0 |
| $e^+ \omega$ | 18 | 18 | 56 | 46 | 19 | 21 | 25 | 26 |
| $\nu_e^c \pi^+$ | 12 | 15 | 3 | 5 | 11 | 14 | 16 | 15 |
| $\nu_e^c \rho^+$ | 6 | 1 | 8 | 7 | 8 | 1.0 | 2.6 | 4 |
| $\mu^+ K^0$ | 1 | 19 | — | 7 | .5 | 18 | 8 | 5 |
| $\nu_\mu^c K^+$ | 2 | 0 | — | .5 | — | 0 | .2 | .6 |

(a) Machacek 1979; (b) Gavela *et al.* 1981a, b; (c) Donoghue 1980; (d) Golowich 1980; (e) Din *et al.* 1980; (f) Kane & Karl 1980.

Neutron decay:

| Mode | (a) | (b) | (c) | (d) | (e) | | |
|------------------|-----|-----|-----|-----|-----|-----|-----|
| | REC | NR | R | R | NR | REC | R |
| $\nu_e^c \pi^0$ | 5 | 8 | 2 | 3 | 8 | 7 | 7 |
| $\nu_e^c \rho^0$ | 3 | .5 | 5 | 4 | .6 | 1.2 | 1.8 |
| $\nu_e^c \eta$ | 2 | 1.5 | 1 | — | 1.5 | — | — |
| $\nu_e^c \omega$ | 3 | 3.5 | 14 | 10 | 5 | 5 | 5 |
| $e^+ \pi^-$ | 54 | 74 | 23 | 32 | 79 | 72 | 68 |
| $e^+ \rho^-$ | 27 | 4 | 55 | 48 | 6 | 12 | 19 |
| $\nu_\mu^c K^0$ | 0 | 10 | — | 2 | 1.1 | 3 | 0.6 |

(a) Machacek 1979; (b) Gavela *et al.* 1981a, b; (c) Donoghue 1980; (d) Golowich 1980; (e) Kane & Karl 1980.

See Langacker (1982) for details of references.

The various decay modes of protons and neutrons according to SU(5) are given in Table 2. The range of branching ratios for the different decay modes is due to the differences in the approaches of different authors, and the parameters used by them (Langacker 1982). It is important to note that in the SU(5) model, the dominant lepton secondary in the decays of the proton and the neutron, is the electron and not the muon.

1.2 Grand Unification Monopoles (GUMS)—Catalysed Proton Decays

In his attempt to understand the quantization of electric charge, half a century ago Dirac (1931) had proposed the existence of magnetic monopoles with magnetic charge a multiple of $g = \hbar c/2e = (137/2)e$. Experimental searches over the 50 years since then have not provided any evidence for them. However, the advent of grand unification theories have revived the interest in the field. Breaking of the GU Symmetries down to $SU(3) \times SU(2) \times U(1)$ predicts the existence of the t'Hooft-Polyakov type magnetic monopoles (t'Hooft 1974; Polyakov 1974) with masses of the order of the grand unification mass $10^{16} \text{ GeV}/c^2$, which corresponds to 10^{-8} g —the mass of a bacterium. The GUT monopole, or GUM as it is called, has a long-range magnetic field. However, being a massive quark condensate with a core of 10^{-30} cm or so, it will need to have a state of perfect symmetry that could have existed perhaps only immediately after the big bang, when quarks and leptons would have been identical as also photons, heavy vector bosons and gluons. In such a state the gauge hierarchy gets broken in stages as one proceeds outwards from the core, and the various particles begin to assume their identities. Thus if GUMs are available, they will constitute a wonderful laboratory for exploration of GUT effects.

Rubakov (1981) and independently Callan (1982a, b) have shown that the grand unification monopole, when it passes through matter, can induce proton decay through reactions of the type $M + p \rightarrow Me^+\pi^0, M\mu^+K^0, Me^+\mu^+\mu^-$ etc. The monopole would come out unscathed in the reaction, but would cause the break up of the proton in a manner identical to what happens in proton decay. A surprising feature of this phenomenon that has made it extremely interesting from the point of view of the experimentalist, is that the cross-section according to Rubakov and Callan for this catalysed proton decay is of the same order as a strong interaction cross-section ($\lambda \sim 30 \text{ cm}$ in iron). If this is the case, then multiple decays should be recorded in a few metres of matter traversed by a GUM. Wilczek (1982), however, has suggested that the cross-section may be more like that of a weak interaction.

1.3 Leptoquarks, the Grand Unification Monopoles (GUMS) and the Early Universe

The masses of leptoquarks and GUMs being of the order of or more than $10^{15} \text{ GeV}/c^2$, it is extremely unlikely that these will ever be produced in terrestrial accelerator laboratories. It has been estimated by an enterprising scientist that a linear accelerator for the purpose would have to extend from the earth to the moon. This being the case, the question arises as to whether these super-massive particles remain only as predictions of GUTs, or whether there exists any possibility that they could have been produced at some point of time in the history of the universe and played a role in its

evolution, perhaps, even surviving up to the present time as relics. It turns out that if we believe in the big-bang origin of the universe, then at times less than 10^{-35} s, conditions were suitable for production of these massive particles.

This extrapolation to such small values (over 53 decades of time) is based upon current ideas of the universe that have emerged from a variety of astronomical observations in the different bands of the electromagnetic spectrum. Constrained by observations of the rate of expansion of the universe, the temperature and density of the universal microwave background and the cosmic abundance of light nuclei, and using all of physics relevant to the different stages of the evolution of the universe it has become possible to construct scenarios of what happened immediately after the big bang. This is illustrated in Fig. 3 which is adapted from Schramm (1983). As is evident from it, the astrophysics of what followed the big bang is best described in the language of modern particle physics.

In the time interval between 10^{-43} to 10^{-35} s after the big bang, the temperature of the universe could have been higher than 10^{12} GeV (10^{25} K) and the density greater than 10^{74} g cm⁻³ sufficiently high to produce particles of mass equal to or greater than 10^{15} GeV/c². It is precisely in this interval that the super-heavy particles and the monopoles could have been produced. If they were, two astrophysical puzzles automatically get solved.

Based on the measurement of the microwave background and the estimated amount of matter in the universe, the ratio of the number of photons to baryons is 10^9-10^{10} ; the universe is dominated by radiation rather than matter. Also, all attempts to detect antimatter in the primary cosmic radiation have resulted only in setting upper limits, clearly showing that in the universe matter dominates over antimatter. In the framework of GUTs, both these large-scale asymmetries can be explained on the basis of a perfectly symmetric origin of the universe. In one of the typical models, it is assumed that initially the massive *X*, *Y* particles and their antiparticles were produced in equal numbers; their decays led to creation of quarks and leptons and their antiparticles. As the temperature

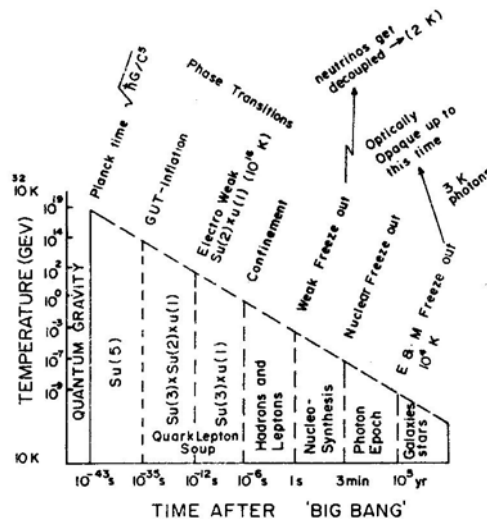


Figure 3. Physics immediately after the big bang at different time intervals—symmetry breaking and phase transitions.

fell, nucleons and antinucleons were produced but not in exactly equal numbers. Their annihilation produced the observed background radiation, and the excess baryons which survived constitute the matter observed now in the universe. By a suitable adjustment of asymmetry in the decay of the X, Y particles and their antiparticles, and introducing in addition the violation of CP symmetry, the observed photon-to-baryon ratio as well as the limits on the matter-to-antimatter ratio can be explained.

In the early universe, super-heavy magnetic monopoles would also have been produced during the symmetry breaking phase transitions. The only way these monopoles could have disappeared is by $M\bar{M}$ annihilation, but a fraction could have survived. It is therefore very important to search for monopoles and measure their flux. Their detection would be of tremendous significance for both physics and astrophysics.

1.4 Super-Unification—SUSYGUTs

In the grand unified theory, the strong, electromagnetic and weak forces are unified as also quarks and leptons. A natural extension of this would be to bring gravity also into the same fold. In molecular, atomic and nuclear phenomena, the role of gravity is insignificant compared to that of the other three forces. But as we have seen, extrapolation to the early universe leads us to a situation where the density becomes enormously high even compared to nuclear densities. Thus at less than 10^{-43} s, quantum gravity effects must also come into play and will require a quantum theory of gravity.

One promising attempt in this direction is the supergravity theory. In it, supersymmetry, *i.e.* the symmetry between fermions and bosons, is introduced as a gauge symmetry. As a consequence, boson partners of all fermions must exist and vice-versa. Thus the super-unification of supergravity with a GUT (SUSYGUT) necessarily leads to new spin $\frac{1}{2}$ fermionic partners for all bosons including the gauge and Higgs bosons. It also predicts new spin 0 particles corresponding to quarks and leptons which have been christened squarks and sleptons. In SUSYGUTs the proton decay lifetime may be extended to 10^{32} yr and even beyond. In the simplest supersymmetric SU(5) type theories, the dominant nucleon decay modes will be $p \rightarrow \tilde{\nu}K^+, \tilde{\nu}_\tau K^+, n \rightarrow \tilde{\nu}_\mu K^0, \tilde{\nu}_\tau K^0$, while the decay modes $e^+\pi, e^+K, \mu^+\pi, \nu\pi$, *etc.* will be suppressed compared to the predictions of the earlier models.

2. Design of proton decay experiments

The design of proton-decay experiments depend on (1) the estimated lifetime, (2) the decay modes and the energy distribution among the secondaries, (3) the background events that stimulate proton decay.

If we take the lifetime as about 10^{30} yr, then one proton will decay in 30 tons of matter per year. Clearly, to cover the predicted range 10^{29} – 10^{32} yr the sensitive mass of the proton-decay detector should be several hundred to several thousand tons.

As we have seen in the SU(5) type model the dominant decay mode is $p \rightarrow e^+\pi^0$, with the electron carrying an energy of about 460 Me V and the individual γ rays which result from the π^0 decay, carrying 240 Me V each. The configuration of the event will be a cascade of 460 Me V due to the electron in one direction and two cascades in the

opposite direction, typically of 240 Me V each with an opening of $\sim 40^\circ$. On the other hand, if we consider a decay mode of the type $p \rightarrow e^+ \omega^0$, where $\omega^0 \rightarrow \pi^+ \pi^- \pi^0$, then the energies are 145 Me V for the electron, 240 Me V each for π^+ and π^- , and 135 Me V each for 2γ rays that result from $\pi^0 \rightarrow 2\gamma$. The configuration of the event will appear isotropic without any forward-backward peaking of tracks. The π^+ will give rise to the decay chain $\pi^+ \rightarrow \mu^+ \nu_\mu$, $\mu^+ \rightarrow e^+ \nu_e \nu_\mu$. Thus μ - e decay can be recorded by measurement of delay in the 0.5–10 μ s range. The decay mode $p \rightarrow \mu^+ \pi^0$ will have the muon of energy of 465 Me V in one direction and a double cascade with an opening angle of 40° in the diametrically opposite direction.

The main background in proton decay experiments is from cosmic-ray secondaries produced in the atmosphere. By installing the detectors deep underground, these effects can be minimised. Clearly, the deeper one is able to go the better is the elimination of these effects, especially those due to muons. However, the intensity of the more serious background due to cosmic-ray-produced neutrinos does not decrease by going to large depths. The background problem has been thoroughly discussed in the papers by Krishnaswamy *et al.* (1982a, b). It is shown there that for dominant decay modes such as $p \rightarrow e^+ \pi^0$, $e^+ \omega^0$, (ρ^0) and $n \rightarrow e^+ \pi^-$, $e^+ \rho^-$ etc. the background will be entirely due to inelastic interactions of neutrinos of a few Ge V energy. The rate of such events is estimated to be one event per year in 60 tons of active detector at equatorial latitudes and a factor of 1.5 higher at higher latitudes ($\lambda > 35^\circ$). This background rate reduces by a factor of 10 if the back-to-back configuration of the events in the decay modes of the type $p \rightarrow e^+ \pi^0$ are clearly established.

3. Dedicated proton decay experiments

Two different approaches have been employed in the experiments that are currently operational to detect proton decay.

3.1 Fine Grain Calorimeters

In the first method, the source of protons and neutrons are the iron nuclei in stacks of iron plates and iron and other nuclei in concrete blocks interspersed in a matrix of either proportional counters or gas discharge tubes, as in the experimental set-ups of KGF (Krishnaswamy *et al.* 1981, 1982a, b, 1983a, b), NUSEX (Battistoni *et al.* 1982, 1983) and Soudan Groups (Peterson *et al.* 1983; Bartlet *et al.* 1983). In these experiments the individual tracks of the secondaries and the cascade electrons are recorded and a complete re-construction of the configuration of the event to good accuracy is feasible. The total energy is determined from the range of the tracks and in the case of soft cascades from the total track length. One of the disadvantages of high-atomic-number materials like iron is that the decay products—the pions and the kaons—either get absorbed in the nucleus itself or get appreciably scattered. The back-to-back configuration of tracks typical of two-body decay is thus distorted to a certain extent. The deviation from 180° could be as much as $\pm 40^\circ$.

The KGF detector set-up at a depth of 7600 m.w.e. (metres water-equivalent) and operating since 1980 November, comprises of 34 layers of proportional counters (1600 in all) with 1.2-cm thick iron plates in between. The total weight of iron is about 140 tons inclusive of the iron walls of the counters. The counters have a cross-sectional area

of $10\text{ cm} \times 10\text{ cm}$ and are 6 m long in the case of counters laid parallel to the walls of the tunnel and 4 m in the case of the alternate layers placed orthogonal to these. From each counter triggered, the ionisation is measured over the range $\frac{1}{3}I_{\min}$ to $100I_{\min}$. Since 1982 December, timing information has been available to an accuracy of 0.5 microseconds which enables the identification of μ_e decays associated with the triggered event.

The NUSEX detector operating in the Mont Blanc tunnel since 1981 August is at a depth of 5000 m.w.e. It has 134 horizontal slabs of iron each of thickness 1 cm and of surface area $3.5\text{ m} \times 3.5\text{ m}$, interleaved with planes of extruded plastic tubes each $1\text{ cm} \times 1\text{ cm}$ in cross section and filled with CO_2 and N-pentane operated in the limited streamer mode. The total weight of the assembly is about 160 tons.

The SOUDAN I experiment installed at a depth of 1800 m.w.e. has been operating since 1981 October. It has 3456 proportional counters each of diameter 2.8 cm and length 2.9 m arranged in 48 layers with 4 cm spacing and embedded in a taconite concrete block of dimensions $3\text{ m} \times 3\text{ m} \times 2\text{ m}$. It has a total mass of 31 tons.

3.2 Water Cerenkov Detectors

In the second method adopted by one Japanese and two U.S. groups, the source of protons and neutrons is the particle detector itself, a large tank of water. The principle of the method is illustrated in the Fig. 4. Let us consider the decay mode $p \rightarrow e^+ \pi^0$. The electron will produce a small cascade which gives rise to a cone of Cerenkov radiation as illustrated. Similarly, the two γ rays that result from the π^0 decay give rise to two cones of radiation in the opposite direction with an angle of $\sim 40^\circ$ between them. From the configuration of the photomultipliers and the amplitudes of light pulses the details of the events such as the location of the vertex, the energy of the secondaries and the relative angles between them can be worked out. One clear advantage of the Cerenkov method is that the direction of the particles can be determined unambiguously. The main disadvantage is that only particles above the threshold velocity will give rise to

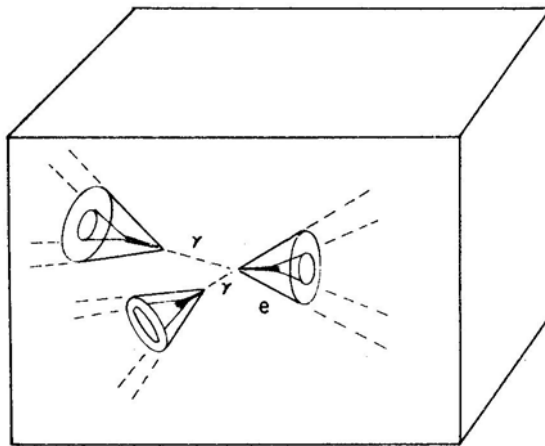


Figure 4. Illustration of the principle of water Cerenkov detector for proton decay. In the decay mode $p \rightarrow e^+ \pi^0$, three cones of light will be produced in the water due to the development of cascades by the positron and the two γ -rays from the decay of π^0 .

Cerenkov radiation and therefore the method is not efficient for some of the decay modes. In a medium like water 80 per cent of the decays will take place in oxygen nuclei and they suffer from the same disadvantage as in iron nuclei discussed earlier. However, the remaining 20 per cent of the decays take place in hydrogen and the secondaries do not suffer the nuclear effects.

In the IMB experiment (Bionta *et al.* 1982) set up at a depth of 1570 m.w.e. in the Morton Salt Mine near Cleveland, Ohio, the water tank has dimensions $22.5 \text{ m} \times 17 \text{ m} \times 18 \text{ m}$ and holds 8000 tons of water. All the six faces of the tank are lined with photomultipliers of 12.5 cm diameter and spaced 1 metre apart (Fig. 5). In all, there are 2048 photomultipliers. The times of arrival of light at the different photomultipliers are recorded to an accuracy of 11 nanoseconds. The accuracy of vertex position determination is about $\pm 60 \text{ cm}$, and the opening angle uncertainty is $\pm 15^\circ$. The energy estimate is accurate to $\pm 10 \text{ per cent}$.

The HPW experiment (Cline 1982) is set up in the Silver King Mine near Park City, Utah, with an overburden of rock 1600 m.w.e. The cylindrical tank (38 ft diameter and 24 ft high) holds 800 tons of water. 704 photomultipliers are distributed throughout the volume of the water. The relative look angle of the photomultipliers are so adjusted that the full 4π solid angle is covered for any event occurring anywhere in the central fiducial

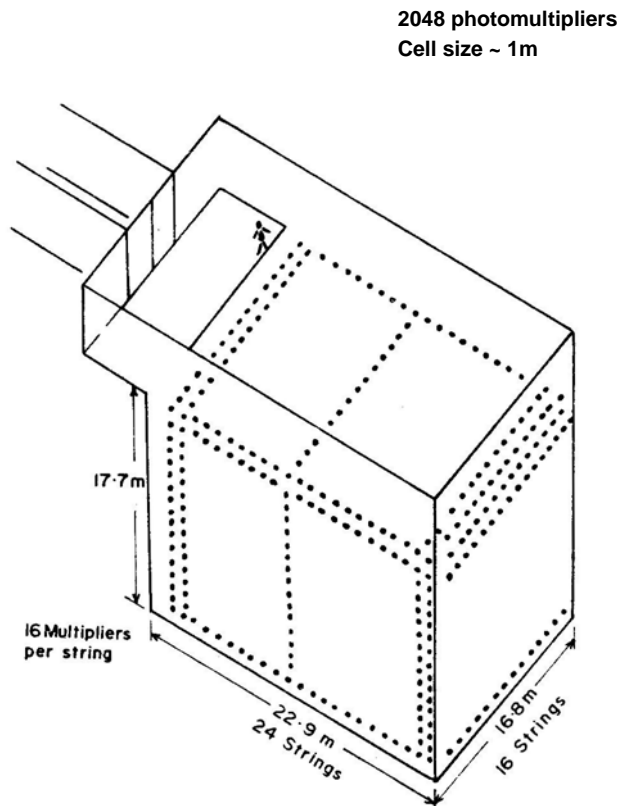


Figure 5. Details of the IMB water Cerenkov detector operating in the Morton salt mines at Fair Port, Ohio at a depth of 1600 m.w.e.

volume. The estimated accuracy of vertex location is 12–40 cm, the decay angle $\sim 14^\circ$ and energy resolution ~ 20 per cent.

The Kamioka proton decay detector (A. Arisaka *et al.* 1984, personal communication) is located in a Zn/Pb mine, 300 km west of Tokyo where the rock overburden is 2700 m.w.e. The capacity of the water tank is 3000 tons, and the fiducial mass 1000 tons. The 1050 photomultipliers with a spherical cathode, specially designed by the Hamamatsu company in Japan are each 20 inches in diameter. A unique feature is that 20 percent of the walls are covered by photomultipliers compared to 1 percent in the IMB experiment. Timing information is available only in the microsecond region and enables the identification of the associated μ - e decay events with 70 per cent efficiency.

4. Results from proton decay experiments

The status of results from the different experiments till 1983 August may be summarised as follows:

The K.G.F. experiment (Krishnaswamy *et al.* 1983a, b) operating since 1980 November has reported three partially confined and three fully confined events, the details of which are given in Table 3. Orthogonal views of the three fully confined and one unconfined event are given in Fig. 6. The cut-away diagrams of events No. 587 (Fig. 7) and 877 (Fig. 8) illustrate the details available for each event.

Among these, event 587 has a high probability of being a neutrino interaction if it is interpreted as a single cascade. However, the detailed features favour the interpretation in terms of two cascades developing in opposite directions in which case the probability for the event to be a neutrino interaction is reduced by a factor of 10.

Event 877 is the strongest candidate for nucleon decay. It has one non-showering track of range 135 g cm^{-2} and in the opposite direction either a shower or a pair of charged particles. In the first case it is consistent with the decay mode $n \rightarrow e^+ \pi^-$ and in the second case with the interpretation $p \rightarrow \mu^+ K_s^0$ with $K_s^0 \rightarrow \pi^+ \pi^-$.

Event 867 is a single non-showering track suffering a large-angle scattering of 37° . The track could be a pion of 450 MeV corresponding to the decay mode $p \rightarrow \nu \pi^{\text{ch}}$ or a kaon of 650 MeV corresponding to $p \rightarrow \nu K^{\text{ch}}$ and $K^{\text{ch}} \rightarrow \mu^{\text{ch}} \nu$. On the basis of these three events, the lifetime is estimated as $\tau/BR \sim 1.7 \times 10^{31}$ yr. These limits are based on 60 tons fiducial mass and 1.9 yr operation. The neutrino background simulating these events is estimated to be less than 0.3, compared to the observed 3 events.

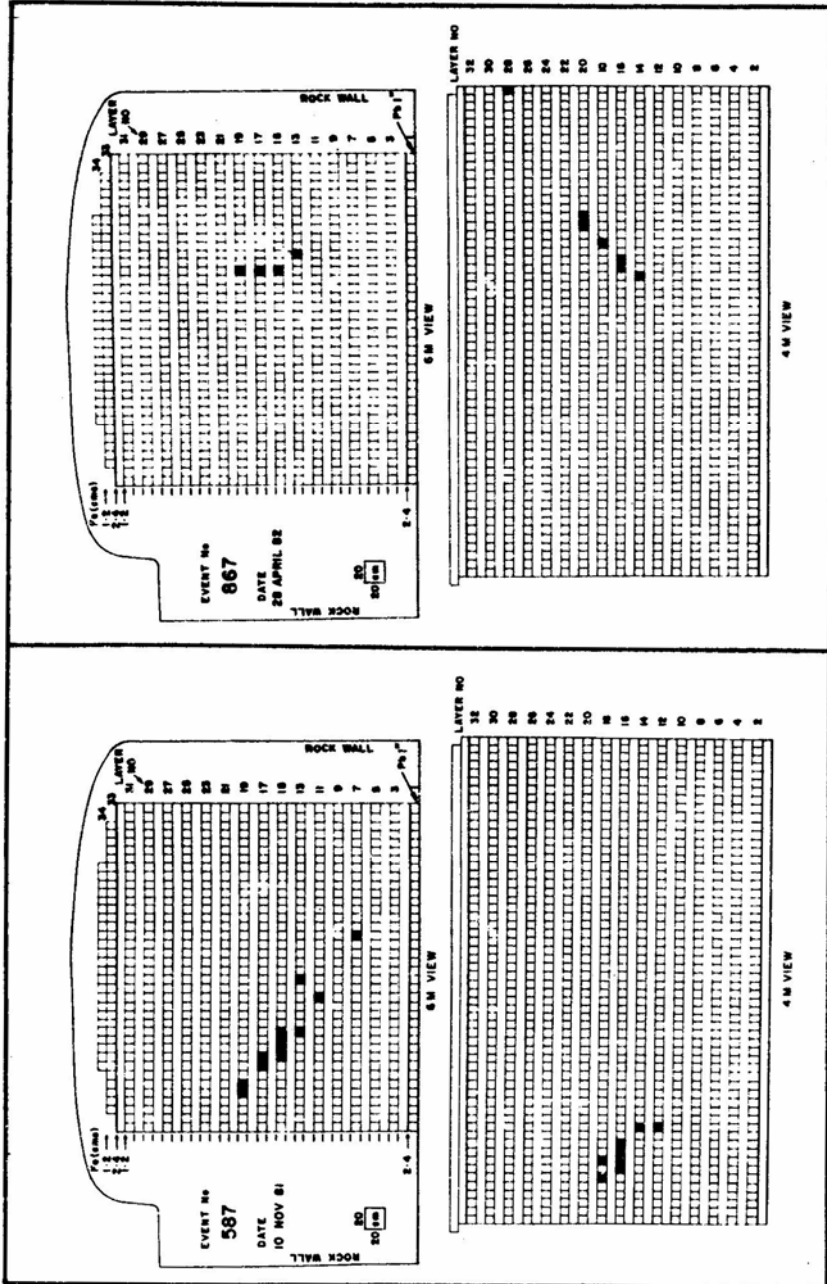
In the Mont Blanc experiment (64 tons fiducial mass, operation time 8 months) 5 fully confined events with a total track length in iron > 10 cm were recorded. The first four events have been interpreted as neutrino interactions. The fifth event cannot easily be interpreted as a neutrino interaction, or as a neutron interaction with any significant probability.

The SOUDAN I experiment with 31.5 tons of iron-loaded concrete has observed one fully confined event in 0.48 years of operation. The estimated total energy of the event is 650 ± 250 MeV. The event appears to have two prongs at about 135° to each other. The absence of hits in counters in certain intermediate layers suggest that part of the event is an electromagnetic cascade. Monte-Carlo simulations by the Soudan group show that the spread in the observation energy of nucleon decay events could be 820–940 MeV depending on the decay mode. The event therefore is consistent with a nucleon decay resulting in two-prong emission.

Table 3. Summary of all the candidate events for nucleon decay recorded in the KGF experiment.

| Event no. | Decay mode | Particle range (g cm^{-2}) | Energy estimates (MeV) ^a | Other plausible modes | ν -background events/1.3 yr |
|----------------------------------|---|---|--|---|---------------------------------|
| fully confined events | | | | | |
| 587 | $p \rightarrow e^+ \pi^0$ | $e^+ \sim 115$ $\pi^0 \sim 150$ | $U_e \sim 500$ $U_{\pi^0} \sim 500$ $U_{\pi^+} \sim 435$ | — | $< 0.5^b$ |
| 867 | $p \rightarrow \bar{\nu} \pi^+$ | $ABC(\pi^+) \sim 182$ | | $p \rightarrow \nu K^+$ $\downarrow \mu^+ \nu \mu$ $p \rightarrow \mu^+ + K_s^0$ $\downarrow \pi^+ \pi^-$ | < 0.05 |
| 877 | $n \rightarrow e^+ \pi^-$ | $AB(e^+):104$ $BC(\pi^-):135$ | $U_e \sim 400$ $U_{\pi^-} \sim 450$ | $U_{\mu} \sim 340 \text{ MeV}$ $U_{\pi^\pm} \sim 320, 220 \text{ MeV}$ | < 0.05 |
| partially confined events | | | | | |
| 87 | $n \rightarrow e^+ \pi^-$ | c | $U_{e^+} \geq 500$ $U_{\pi^-} \sim 400$ $E_{\text{all}} > 540$ | $p \rightarrow e^+ \pi^0 (2\gamma)$ $U(\gamma_1) \quad U(\gamma_2)$ $p \rightarrow \mu + K_s^0$ $\downarrow \pi^+ \pi^-$ | < 0.05 |
| 251 | $p \rightarrow e^+ \rho^0$ | c | | | < 0.05 |
| 722 | $p \rightarrow e^+ \omega^0 \rightarrow 3\pi$ | A: ~ 52 B: > 170 C: ~ 15 D(e^+): ~ 10 | $E_A \sim 245$ $E_B \sim 335$ $E_C \sim 55$ $E_D \sim 80$ | — | < 0.2 |

^a The symbols E and U refer to visible energy loss (excluding particle mass) and the total energy respectively. ^b Estimated rate for single cascade. It would be much lower for the preferred interpretation of two cascades starting at the mid-point of the event. ^c See Krishnaswamy *et al.* (1981).



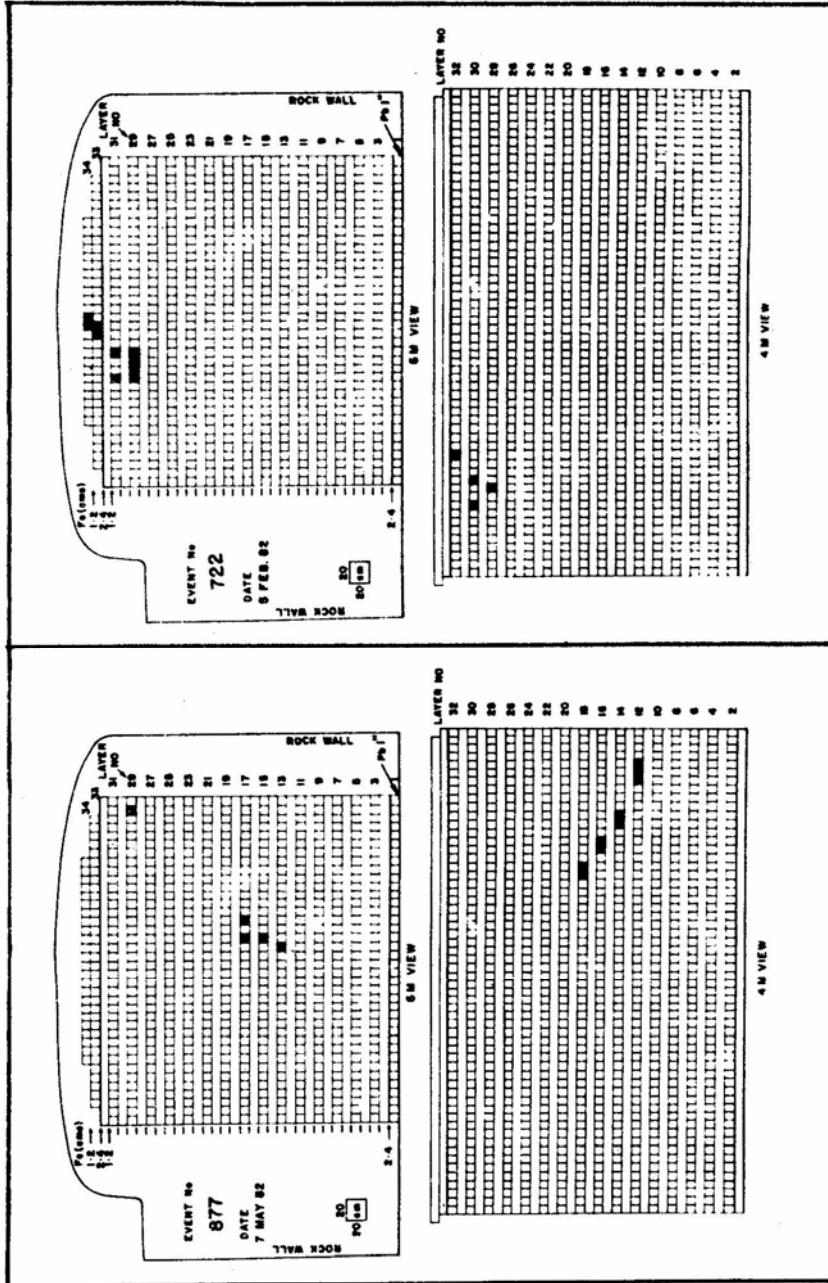


Figure 6. The two orthogonal views of the fully confined events No. 587, 867 and 877 and one partially confined event No. 722 in the KGF proton decay detector. Each black square represents one counter triggered above the threshold value. The full details of the events 587 and 877 are given in Figs 7 and 8.

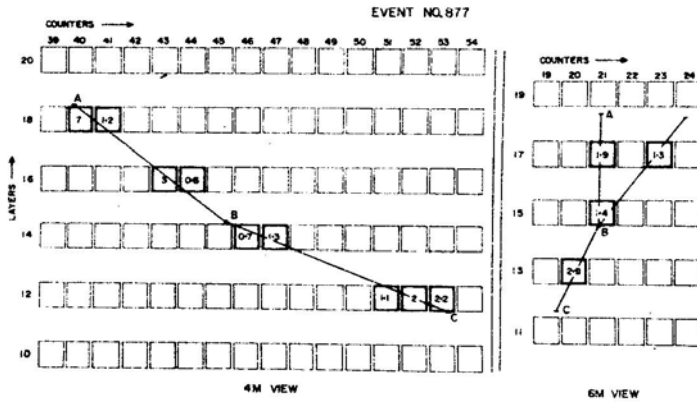


Figure 7. The cut-away diagram of event No. 587. The numbers within the squares give the ionisation recorded in the counters in terms of the ionisation of a vertical minimum ionising particle. The lines indicate the plausible configuration of the event consistent with the interpretation of $p \rightarrow e^+ \pi^0$, $\pi^0 \rightarrow 2\gamma$. The shower seen in the layers 15–19 corresponds to e^+ with energy ~ 500 Me V while the two photons with energy ~ 200 and 300 Me V give rise to the shower in the downward direction for layer 15.

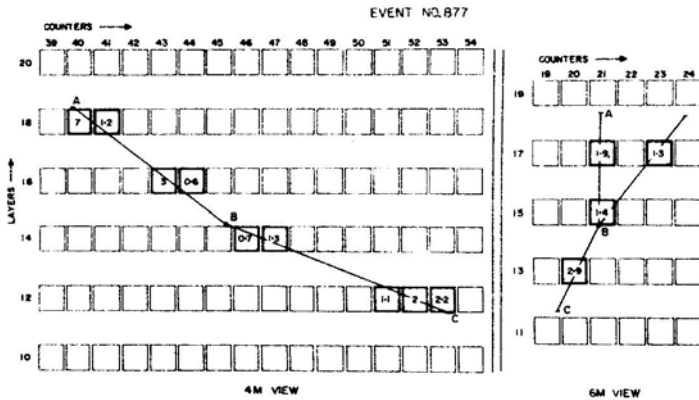


Figure 8. The cut-away view of event No. 877. Two alternative interpretations have been given by the authors (Krishnaswamy *et al.* 1982a, b): (i) $n \rightarrow e^+ \pi^-$. The shower AB is due to the positron e^+ and the track BC the charged pion, (ii) $p \rightarrow \mu^+ K_S^0$. The track BC is due to μ^+ (350 Me V) and the upward-forked branches correspond to two pions π^+ , π^- (320, 220 Me V) from the decay of K_S^0 .

In the IMB experiment, in the first 80 days of operation with a fiducial mass of 3300 ions, 69 fully confined events were recorded with at least 45 photomultipliers recording above threshold in each event. Within the statistical accuracy, the above events were uniform in vertex position and isotropic in track direction. The fraction of fully contained events with μ - e decay signature was 0.4 ± 0.1 after correcting for detection efficiency.

The characteristics of the 69 confined events have been summarised as follows:

(1) 66 single or multi-track events which do not possess a track lighting more than 40

tubes in the backward hemisphere and hence are outside the angle and energy requirements for $p \rightarrow e^+ \pi^0$.

(2) Two wide-angle track events both of which are associated with μ - e decay and hence do not qualify as $p \rightarrow e^+ \pi^0$.

(3) One two-track event in which the total number of photomultiplier hit were 340 about a factor of 2 greater than expected for $p \rightarrow e^+ \pi^0$. Also the opening angle was $115 \pm 15^\circ$ outside the predicted range ($> 140^\circ$) for free or bound proton decays in the mode $e^+ \pi^0$.

Since there is no candidate, $\tau/BR > 6.5 \times 10^{31}$ yr for (free + bound) and $\tau/BR > 1.9 \times 10^{31}$ yr for free protons only.

Since no candidate events have been seen even in a further analysis of data of 130 days operation, these limits have been pushed to $> 10^{32}$ yr for all and $> 6.5 \times 10^{31}$ yr for protons only.

At the recent ICOBAN 84 (International Colloquium on Baryon Non-conservation) held at Park City, Utah in January 1984, several groups presented candidates for nucleon decay with due reservation and caution.

The first results based on 176 days of operation from 1983 July 6 were presented by the Kamioka group, corresponding to 324 ton-years. Out of a total of 65726 events selected for visual scan and analysis, 57 events were in the fiducial volume, 40 with single rings and 17 with multiple rings (rings of light are produced when the Cerenkov cones intercept the walls of photomultipliers). Out of the 40 single rings, two had the characteristics to be interpreted as $p \rightarrow \nu K^{\text{ch}}$ with $K^{\text{ch}} \rightarrow \mu^{\text{ch}} \nu$. Out of the 17 multiple ring events one three-ring event could be a case of $p \rightarrow \mu^+ \eta$ or μK^0 ($K^0 \rightarrow 2\pi^0$) or $n \rightarrow e^+ \rho^-$ ($\rho^- \rightarrow \pi^- \pi^0$) and one five-ring event that could be $p \rightarrow e^+ \omega^0$ or $n \rightarrow e^+ \rho^-$. The experiment sets a lower limit of $\tau/BR = 2.6 \times 10^{31}$ yr for $p \rightarrow e^+ \pi^0$ decay mode.

In the HPW experiment, one candidate event with two muons which could be a case of $p \rightarrow \mu^+ K^0$, $K^0 \rightarrow \pi^+ \pi^-$ and $\pi^+ \rightarrow \mu^+ \nu_\mu$ has been seen.

NUSEX have reported a new event which could either be $p \rightarrow e^+ \pi^0$ or a neutrino interaction $\nu_e \rightarrow e$.

In the KGF experiment, a fourth confined event has been seen which could be interpreted as either $n \rightarrow \nu \eta^0$, $\eta^0 \rightarrow 3\pi^0$ or $n \rightarrow e^+ \rho^-$, $\rho^- \rightarrow \pi^- \pi^0$.

In the light of all this, what seems clear is that the lifetime for the decay of a nucleon is higher than 10^{31} yr and the dominant decay mode is not $e^+ \pi^0$. If the lifetime were of the order of 10^{29} to 10^{30} yr and the dominant mode $e^+ \pi^0$, then, by now several of the experiments already in operation would have established the decay without any ambiguity. Looking at the candidate events reported by the different groups, it is perhaps possible that decay modes with muon as one of the secondaries may equal or even have a higher probability than electron secondaries.

The reservation and caution in the interpretation of the events as candidates for nucleon decay stem from the fact that there is no unique signature for decay that cannot be simulated by a neutrino interaction. The total energy of the event (940 Me V) and the back-to-back configuration are the two chief characteristics that have been used to reduce the probability of a candidate event from being a neutrino interaction. In these circumstances it has to be recognised that the nucleon decay phenomenon will not be established on the basis of clear-cut individual events that can have no other explanation, as happened in the case of discoveries of various fundamental particles and their decays. The final proof has to come on the basis of a large number of events which, in the energy spectrum plot of neutrino-induced events, will stand out unambiguously

around 1 Ge V energy. From this point of view, it is necessary to have good energy resolution, angular resolution and good rate of candidate events. Consistent with the high rate of potential events, it is unlikely that the energy and angular resolution can be improved beyond what has been achieved with the IMB and Kamioka set ups as far as water Cerenkov detectors are concerned.

The situation with regard to the fine-grain calorimeters is not quite the same. There is considerable scope for improvement in this type of detectors.

The Frejus experiment, which is a collaboration between Orsay, Palaseau, Saclay and Wuppertal (Barloutaud 1982, 1983) and is to go into operation in 1984 in the Modane underground laboratory (4500 m.w.e.) east of Grenoble in France, is a step in this direction. The detector is a fine-grain calorimeter made up of $0.5 \text{ cm} \times 0.5 \text{ cm} \times 6 \text{ m}$ flash tubes and 3-mm thick iron plates with Geiger counters of cross-sectional area $1.5 \text{ cm} \times 1.5 \text{ cm}$ interspersed in the stack every one metre and will serve as the triggering detectors. The total mass of iron will be 1.5 kilo-tons. Because of the fine-grain nature, the directions of muons for example from kaon decay can be measured by the increase in multiple scattering, and the positrons from μ^+ decay can be seen by using a long HT pulse on the flash chambers. The energy resolution expected is 12–20 per cent for pions of 200–300 Me V. Nucleon decay experiments planned for the future have been reviewed by Grant (1983). The second phase of the KGF experiment, the Soudan II and the Grand Sasso project will all incorporate improved, larger versions of fine-grain calorimeters. Liquid scintillation counters, high-pressure and liquid-argon detectors working in TPC-like modes, and even a 3000-ton liquid-argon bubble with 50 per cent duty cycle have been under consideration to achieve the requisite fine structure and energy resolution.

5. Limits on flux of superheavy magnetic monopoles (GUMs)

Excepting in the experiment of Cabrera (1982) in which the magnetic monopole is detected by the change in magnetic flux as it passes through a superconducting ring, all other experiments that have been carried out recently depend on the velocity of the

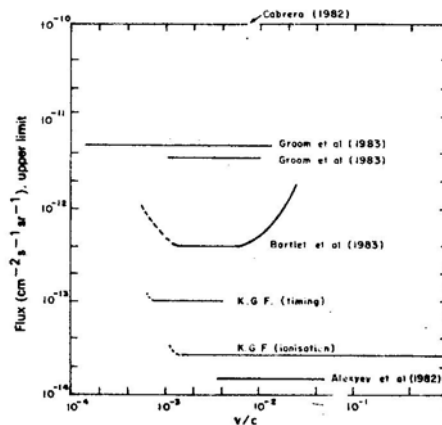


Figure 9. Comparison of the upper limits on the flux of GUT monopoles in various experiments as a function of velocity.

magnetic pole and its ionisation characteristics. They are therefore sensitive only in certain velocity ranges. Cabrera's first experiment carried out with a superconducting loop of area 20 cm^2 gave evidence of one candidate in an operating period of 151 days which corresponds to a velocity independent flux limit of $6.1 \times 10^{-10} \text{ cm}^{-2} \text{ s}^{-1} \text{ sr}^{-1}$. In a subsequent experiment Cabrera *et al.* (1983), using a three-loop superconducting device of effective area 476 cm^2 , did not find any candidate in 150 days of operation thus setting an upper limit of $3.7 \times 10^{-11} \text{ cm}^{-2} \text{ s}^{-1} \text{ sr}^{-1}$.

The limits set by different experiments (Groom *et al.* 1983, Bartlet *et al.* 1983, Krishnaswamy *et al.* 1983a, b, Alexeyev *et al.* 1983) sensitive to different velocity ranges are shown in Fig. 9. It is clear that the flux in the velocity range $10^{-3} c$ to c is less than $2 \times 10^{-14} \text{ cm}^{-2} \text{ s}^{-1} \text{ sr}^{-1}$ at least three orders of magnitude lower than the limit to the velocity independent flux given by Cabrera *et al.* The experiments will soon be able to reach the bound of $10^{-16} \text{ cm}^{-2} \text{ s}^{-1} \text{ sr}^{-1}$ set by Parker (1970) on the basis of the existence of a galactic magnetic field.

5.1 Monopole Catalysis of Nucleon Decay

Searches for super-heavy magnetic monopoles catalysing nucleon decay have been made with practically all the nucleon-decay experiments in progress. In the IMB experiment, in 100 days of operation, no event was recorded that satisfied the criteria of multiple nucleon decays from the passage of a magnetic monopole. Fig. 10 shows the upper limit (90 per cent confidence) on monopole flux for different velocities as a function of the catalysis cross-section. In the KGF detector, a chain of nucleon decays can be seen if the second and subsequent events occur within $7 \mu\text{s}$ of the trigger, and the separation between the decays is less than the dimensions of the detector. In 2.52 years

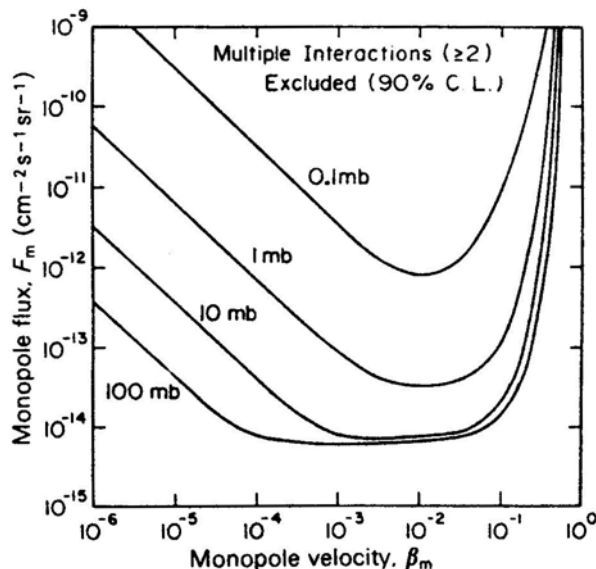


Figure 10. Limits on monopole flux deduced from the IMB experiment on the basis of Rubakov-Callan effect and different cross-sections for induced decay (Bionta *et al.* 1982).

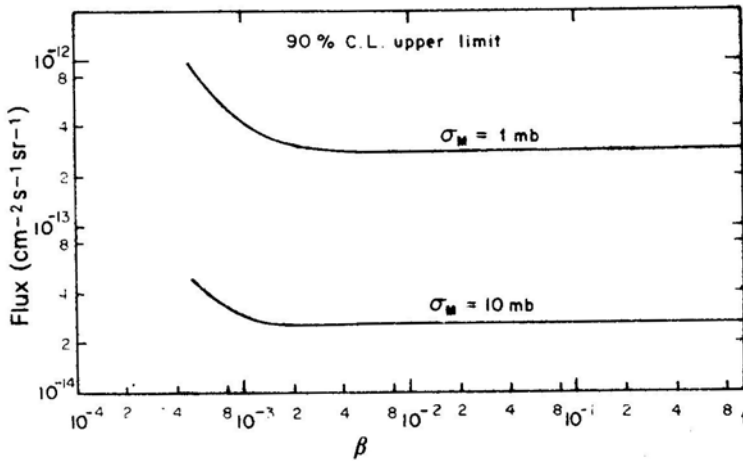


Figure 11. Limits on the monopole flux deduced from the KCF experiment based on two values for induced proton decay (Krishnaswamy *et al.* 1983a, b)

of operation there is no evidence for chains of two or more than two decays. Fig. 11 shows the 90 per cent confidence upper limit on the monopole flux for chain decays as a function of velocity and for two values of catalysis cross-section, 10 mb and 1 mb.

6. Conclusion

In conclusion, as of 1984 January, it may be stated that the existence of super-heavy monopoles and the phenomenon of nucleon decay, both of which are extremely important from the point of view of grand unification theories, are still very open questions. While there has been just one magnetic monopole candidate so far, there have been several as far as nucleon decay is concerned. The first candidates for nucleon decay came from the fine-grain calorimeters of KGF, and NUSEX; recently there have been candidates from the water Cerenkov experiments as well. The experimental situation regarding the other important phenomena of relevance to grand unification which we have not discussed in this article—like the finite mass of neutrinos, neutrino oscillations, and neutron oscillations—continues to be indefinite though many dedicated experiments are in progress.

With the continued operation of the nucleon decay experiments already collecting data and the commissioning of the new generation of experiments over the next few years, the stage is set for a resolution of this problem in a time scale of 5–10 years. The present indication that the dominant decay mode for the proton (even if it decays) is not $p \rightarrow e^+ \pi^0$ and that the lower limit to the lifetime of the nucleon is 10^{31} yr, does not favour the simple SU(5) type models.

The remarkable discoveries of W^\pm and Z^0 with mass values exactly as predicted, have given a boost to the unification based on the gauge theoretical approaches. Whether grand unification can be extended to super-unification, experiment alone can tell. This will be the challenge for the remaining years of this century.

Acknowledgement

I would like to express my thanks to Professor V. S. Narasimham for helpful discussions.

References

- Alexeyev, E. N., Boliev, M. M., Chudakov, A. E., Makoev, B. A., Mikheyev, S. P., Sten'kin, Yu, V. 1982, *Lett. Nuovo Cimento*, **35**, 413.
- Bartlet, J. *et al.* 1983, *Phys. Rev. Lett.*, **50**, 651.
- Barloutaud, R. 1982, in *Int. Coll. Baryon Nonconservation*, Eds V. S. Narasimham, P. Roy, K. V. L. Sarma, B. V. Sreekantan, Indian Academy of Sciences, Bangalore, p. 143.
- Barloutaud, R. 1983, in *Int. Coll. Matter Nonconservation*, INFN, Rome, p. 177.
- Battistoni, G. *et al.* 1982, in *Int. Coll. Baryon Nonconservation*, Eds V. S. Narasimham, P. Roy, K. V. L. Sarma, B. V. Sreekantan, Indian Academy of Sciences, Bangalore, p. 83.
- Battistoni, G. *et al.* 1983, in *Int. Coll. Matter Nonconservation*, INFN, Rome, p. 107.
- Bionta, R. M. *et al.* 1982, in *Int. Coll. Baryon Nonconservation*, Eds V. S. Narasimham, P. Roy, K. V. L. Sarma, B. V. Sreekantan, Indian Academy of Sciences, Bangalore, p. 137.
- Cabrera, B. 1982, *Phys. Rev. Lett.*, **48**, 1378.
- Cabrera, B. *et al.* 1983, *Phys. Rev. Lett.*, **51**, 1933.
- Callan, C. G. 1982a, *Phys. Rev.*, **D25**, 2141.
- Callan, C. G. 1982b, *Phys. Rev.*, **D26**, 2058.
- Cline, D. B. 1982, in *Int. Coll. Baryon Nonconservation*, Eds V. S. Narasimham, P. Roy, K. V. L. Sarma, B. V. Sreekantan, Indian Academy of Sciences, Bangalore, p. 99.
- Cobb, J. H. 1983, in *Int. Coll. Matter Nonconservation*, INFN, Rome, p. 88.
- Dirac, P. A. M. 1931, *Proc. R. Soc. London*, **A133**, 60.
- Georgi, H., Glashow, S. L. 1974, *Phys. Rev. Lett.*, **32**, 438.
- Georgi, H., Quinn, H. R., Weinberg, S. 1974, *Phys. Rev. Lett.*, **33**, 451.
- Grant, A. L. 1983, in *Fourth Workshop on Grand Unification*, Birkhäuser, Boston, p. 69.
- Groom, D. E. *et al.* 1983, *Phys. Rev. Lett.*, **50**, 573.
- Krishnaswamy, M. R., Menon, M. G. K., Mondal, N. K., Narasimham, V. S., Sreekantan, B. V., Hayashi, Y., Ito, N., Kawakami, S., Miyake, S. 1981, *Phys. Lett.*, **106B**, 339.
- Krishnaswamy, M. R., Menon, M. G. K., Mondal, N. K., Narasimham, V. S., Sreekantan, B. V., Hayashi, Y., Ito, N., Kawakami, S., Miyake, S. **1982a**, *Pramana*, **19**, 525.
- Krishnaswamy, M. R., Menon, M. G. K., Mondal, N. K., Narasimham, V. S., Sreekantan, B. V., Hayashi, Y., Ito, N., Kawakami, S., Miyake, S. 1982b, *Phys. Lett.*, **115B**, 349.
- Krishnaswamy, M. R., Menon, M. G. K., Mondal, N. K., Narasimham, V. S., Sreekantan, B. V., Hayashi, Y., Ito, N., Kawakami, S., Miyake, S. 1983a, in *Int. Coll. Matter Nonconservation*, INFN, Rome, p. 97.
- Krishnaswamy, M. R. *et al.* 1983b, in *Fourth Workshop on Grand Unification*, Birkhäuser, Boston, p. 25.
- Langacker, P. 1982, in *Int. Conf. Baryon Nonconservation*, Eds V. S. Narasimham, P. Roy, K. V. L. Sarma, B. V. Sreekantan, Indian Academy of Sciences, Bangalore, p. 34.
- Parker, E. N. 1970, *Astrophys. J.*, **160**, 383.
- Pati, J. C. 1983, in *Int. Coll. Matter Nonconservation*, INFN, Rome, p. 45.
- Pati, J. C., Salam, A. 1973, *Phys. Rev. Lett.*, **31**, 661.
- Peterson, E. *et al.* 1983, in *Int. Coll. Matter Nonconservation*, INFN, Rome, p. 80.
- Polyakov, A. M. 1974, *JETP Lett.*, **20**, 194.
- Rubakov, V. A. 1981, *JETP Lett.*, **33**, 644.
- Schramm, D. N. 1983, *Physics Today*, **36**, No. 4, 27.
- t'Hooft, G. 1974, *Nucl. Phys.*, **B79**, 276.
- Wilczek, F. 1982, *Phys. Rev. Lett.*, **48**, 1144.